journal

J. Am. Ceram. Soc., **99** [4] 1449–1454 (2016)
DOI: 10.1111/jace.14119

Effects of Sintering Temperature on Open-Volume Defects and Thermoluminescence of Yttria and Lutetia Ceramics

Matthew G. Chapman,[‡] Roger C. WalkerII,[‡] Jaclyn M. Schmitt,[§] Cameron L. McPherson,[‡] Fnu Ameena,[¶] Courtney J. Kucera,[§] Carroll A. Quarles,[¶] Timothy A. DeVol,[||] John Ballato,[‡,§] and Luiz G. Jacobsohn[‡,§,†]

[‡]Department of Materials Science and Engineering, Clemson University, Clemson, South Carolina 29634

[§]Center for Optical Materials Science and Engineering Technologies (COMSET), Clemson University, Anderson, South Carolina 29625

[¶]Department of Physics and Astronomy, Texas Christian University, Fort Worth, Texas 76129

[||]Environmental Engineering and Earth Sciences Department, Clemson University, Anderson, South Carolina 29625

The effects of different processing steps and processing conditions for the fabrication of Y_2O_3 and Lu_2O_3 ceramics were investigated, particularly the effects of calcination, and sintering temperature on the content of open-volume and electronic defects. Ceramic bodies were prepared from calcined powders by sintering from 1400°C to 1700°C for 20 h. Density was determined by the Archimedes method and showed pellets reached about 99% of Y_2O_3 density for temperatures ≥1450°C, and reached 98% for sintering at 1700°C for Lu_2O_3. The content of open-volume defects was followed by positron annihilation lifetime (PAL) measurements. For both materials, two lifetimes were obtained. The faster lifetime, 211 ps for Y_2O_3 and 204 ps for Lu_2O_3, was assigned to bulk annihilation with possible contribution of grain boundaries. The longer lifetime was assigned to positronium annihilation in open-volume defects with radii of 2–4 Å. Doppler broadening analysis revealed the same type of defect in Lu_2O_3 ceramics for all sintering temperatures. PAL analysis results showed that densification was achieved through the elimination and agglomeration of open-volume defects. Thermoluminescence (TL) measurements of Y_2O_3 showed that sintering is beneficial in eliminating traps and/or recombination centers, and that higher sintering temperatures increase TL signal.

I. Introduction

Transparent ceramics, originally designed for lighting,[1] are now used in a variety of applications that range from transparent armor and infrared windows to lasers and scintillators.[2–5] Scintillators are luminescent materials used for the detection and measurement of ionizing radiation, finding application in many fields, including medical imaging and diagnosis, oil exploration, security, and science. The first transparent ceramic scintillators were fabricated in the mid-1980's, when rare earth (RE)-doped $(YGd)_2O_3$[6] and Gd_2O_2S[7,8] were introduced. These scintillators found enormous commercial success as ionizing radiation sensors in computed tomography (CT) scanners. Recently, Y_2O_3(:RE) and Lu_2O_3:RE have attracted attention as scintillators.[9–15] However, there remains a knowledge gap relating to the fabrication and processing conditions of ceramic scintillators with their scintillation output, a situation that negatively impacts the greater use of these materials, as well as limits their performance. For example, open-volume defects generate light scattering and degrade performance. Likewise, electronic traps capture electrons and/or holes and decrease the yield of radiative recombination at the luminescence center. The fabrication of transparent ceramics involves numerous processing steps each of which impact optical and scintillation performance, from the synthesis of the precursor materials in powder form and their calcination to sintering and eventual hot isostatic pressing (HIP). Recently, the effects of different sintering conditions on the pore content of Sc_2O_3:Er transparent ceramics were investigated using positron annihilation spectroscopy (PAS).[16] Also, it was shown for the case of Y_2O_3:Tm transparent ceramics that postfabrication processing in O_2-rich atmospheres was able to enhance both photoluminescence and scintillation performance concomitant to the reduction in electronic traps as determined by thermoluminescence (TL) measurements.[17] In this work, the effects of different processing steps and processing conditions for the fabrication of Y_2O_3 and Lu_2O_3 ceramics were investigated, particularly the effect of calcination and sintering temperature on the content of open-volume defects, i.e., defects that present void space, including vacancies and pores, and electronic defects by means of the complementary techniques of positron annihilation lifetime (PAL), TL, and density determination.

II. Experimental Procedure

Undoped Y_2O_3 powders were prepared by co-precipitation following an established procedure.[18,19] Briefly introduced here: a 0.25*M* yttrium nitrate solution was prepared by dissolving yttrium nitrate hexahydrate in ultrapure water, a 5*M* solution of ammonium sulfate was added to the nitrate solution, and a 2*M* ammonium hydroxide solution was added dropwise in order to precipitate a yttrium nitrate precursor. The precipitated precursor was maintained for 3 h at room temperature and then washed twice with ultrapure water and ethanol. After the final washing, the precipitate was dried at 60°C overnight under vacuum. The dried precursor was calcined at 1050°C for 4 h under oxygen to yield Y_2O_3, uniaxially pressed into pellets and then cold isostatically pressed at 200 MPa.

Undoped Lu_2O_3 powders were also prepared by co-precipitation.[20] Briefly, a lutetium nitrate solution was prepared by dissolving Lu_2O_3 powder in excess amounts of nitric acid

H. Guo—contributing editor

Manuscript No. 37418. Received August 27, 2015; approved December 12, 2015.
[†]Author to whom correspondence should be addressed. e-mail: luiz@clemson.edu

at approximately 80°C. A 100 mL of 1M ammonium hydroxide solution was dripped into a 100 mL of 0.2M lutetium nitrate solution at a rate of about 5 mL/min in order to precipitate lutetium hydroxide. After homogenizing for an hour, the hydroxide precipitates were separated by centrifugation and then washed several times with water to remove impurities and any remnant salts. Lutetium sulfate with an initial pH value of 2.3 was prepared by dissolving the hydroxyl precipitates with a stoichiometric amount of sulfuric acid. The Lu_2O_3 powders were prepared by dripping a 100 mL of 2M hexamethylenetetramine (HMT) solution into the 100 mL of 0.1M lutetium sulfate solution at a rate of about 5 mL/min under mild stirring at 80°C to accelerate the decomposition of HMT. After homogenizing for an hour, the final pH value of the resultant suspension was 6.6. The precipitates were washed several times with water to remove the byproducts and dried in vacuum oven at 70°C. The precursors were calcined at 1100°C for 4 h under flowing oxygen gas to produce Lu_2O_3 powders, which were then uniaxially pressed into pellets and then cold isostatically pressed under 200 MPa.

Sintering was carried out under vacuum (base pressure in the low 10^{-6} mbar range) for 20 h, at temperatures ranging from 1400°C to 1700°C and a heating rate of 10°C/min. Once completed, samples were allowed to cool naturally to room temperature. Sintered samples are optically opaque, and no difference in transparency/translucency can be observed in the samples.

Density was determined by the Archimedes method using distilled water (density = 1 g/cm^3) and taking 5.031[21] and 9.410[22] g/cm^3 for the intrinsic density of Y_2O_3 and Lu_2O_3, respectively. Results correspond to the average of several measurements of 3 to 4 pellets from a same batch. The error bars correspond to the standard deviation of these measurements.

The PAL was measured in a typical fast–fast coincidence set-up using two Photonis XP2020/URQ photomultiplier tubes (PMTs) with barium fluoride scintillators.[23] The start and stop signals from the PMTs went to Ortec 583 constant fraction differential discriminators which were set to select the 1.27 MeV gamma ray from the ^{22}NaCl source for the start signal and the 511 keV annihilation gamma ray for the stop signal. The signals went to an Ortec time-to-amplitude converter and then to an Ortec Trump multi-channel analyzer (MCA) installed in a computer and operated with the software Maestro. The ^{22}NaCl source, manufactured by Eckert & Ziegler Isotope Products, was deposited on 12.5 μm titanium film, and covered and sealed with a second identical titanium film. The source was placed between two samples from the same batch and the sample–source–sample was sandwiched between two 1.4 mm titanium foils. Based on the density and thickness of the samples, any positrons that made it out of the source were stopped in the sample. Lifetime runs were made to obtain 1 to 8 million events total. In some cases, error bars are smaller than the symbol size.

The lifetime data were analyzed with the program LT (version 9).[24] The resolution function was assumed to be two Gaussian functions and the range of data analyzed extended from a counting level about one tenth of the peak to well into the region of the constant random background. The lifetime data were fit with one or two lifetime components related to the sample together with a source correction determined using the Monte Carlo code MCNP.[25] The source correction consisted of two components, a short component due to both the titanium foil and the ^{22}NaCl source, and the longer component due to the ^{22}NaCl source. The procedure to establish the source correction was to measure the lifetime from the source between the titanium foils alone. The MCNP results were used to determine what fraction of the positron spectrum annihilates in the different parts of the sample–source: the ^{22}NaCl source, the titanium film covering the source and the sample. With the sample–source–sample arrangement used, the contribution to the lifetime spectrum from positrons stopped in the sample was calculated to be 67%. In the analysis of PAL data, two lifetime components for the samples yielded better consistency and better degree of confidence through best fit variance than one lifetime component, and the discussion of PAL results throughout the rest of the manuscript refers to the two lifetimes related to the sample.

The Doppler broadening experiment was performed with the same sample–source–sample arrangement, but with the ^{22}Na source replaced with a ^{68}Ge source, using a liquid nitrogen-cooled high-purity germanium detector (HPGe) which is a 5.08 cm coaxial crystal with an aluminum cover. The output signal was processed by an Ortec 571 amplifier and then sent to a second Trump MCA. In the Doppler broadening experiments, data were collected to obtain 4 million events in the 511 keV peak. The analysis of the Doppler broadening spectrum determines the S and W parameters for the 511 keV gamma ray peak. The S parameter is defined as the ratio of the number of counts within about 1 keV of the 511 peak center to the total number of counts in the peak, while the W parameter corresponded to the ratio of the number of counts in the wings of the peak to the total number of counts in the peak. No correction has been made for positron annihilation in the source.

TL measurements were carried out using a Thermo Scientific Harshaw thermoluminescence dosimeter (TLD) reader model 3500. Samples were heated from 50°C to 400°C at a rate of 25°C/s and held at 400°C for 1 min in order to completely deplete the traps, and then immediately measured from 50°C to 400°C at a rate of 1°C/s to confirm the traps were fully depleted. Samples were then placed in a Rigaku Ultima IV X-ray diffractometer where they were irradiated with Cu$K_{\alpha+\beta}$ X-rays for 2 min. After irradiation, samples were measured from 50°C to 400°C at a rate of 1°C/s and then immediately remeasured to confirm the traps were fully depleted. About 8–12 TL glow curves were obtained for each sintering temperature. Glow curves presented in this work were normalized by the mass of the samples, unless otherwise noted. Since sintered samples have essentially the same thickness and density does not vary much within the sintering temperature range investigated, it is possible to say that within the error of a few % that the correction of TL intensity by the mass of the samples is equivalent to correcting it by the area of the samples. Averages of the areas of the glow curves are presented and the error bars correspond to the standard deviation of these averages.

III. Results and Discussion

(1) Yttria

The presence of open-volume defects in yttria pellets was investigated by density and PAL measurements. Density results are presented in Fig. 1 where densities of about 99% of the reference value (dashed line) were obtained for temperatures ≥1450°C, in agreement with previous results.[26] PAL measurements are based on the fact that the PAL is sensitive to the local electronic density, noting that the electronic density of open-volume defects is lower. The annihilation lifetime also depends on the state of the positron that can be delocalized, while diffusing through the solid after thermalization, trapped in an open-volume defect, or forming a positronium the unstable self-bonded electron–positron pair that is created when a thermalized positron is electrostatically captured by an electron. From these different annihilation conditions, delocalized positron annihilation yields the so-called "bulk" lifetime, while the lifetimes for trapped positron and positronium annihilation are considerably longer. Consequently, analysis of the annihilation lifetime yields information on the presence and relative concentration of open-volume defects of different dimensions.[27] Analysis of PAL results revealed the presence of two lifetimes. The lifetime component values and relative contributions are shown in Fig. 2 as a function of the sintering temperature. The fast component continuously decreased from 227 to 211 ps for higher sintering temperatures and the slow component varied within the 1040–3670 ps range [Fig. 2(a)]. The large variation in the slower lifetime component is a consequence of the effects of the small relative contribution (<1%) of this component in the fitting analysis. The slow component is ascribed to positronium annihilation in open-volume defects.

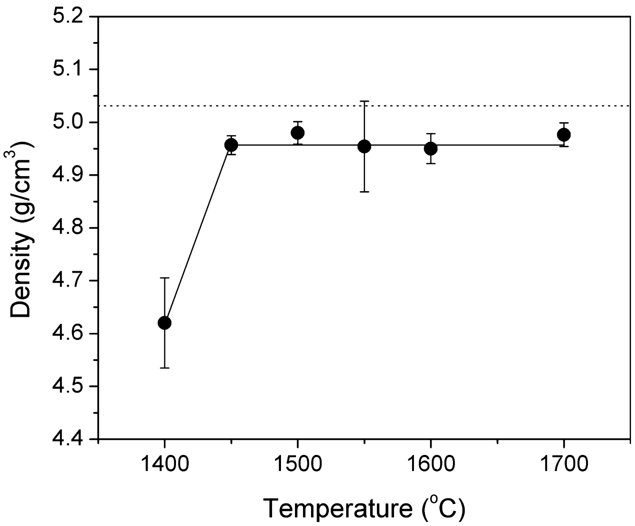

Fig. 1. Density of Y_2O_3 pellets sintered at different temperatures. Line is a guide to the eye only.

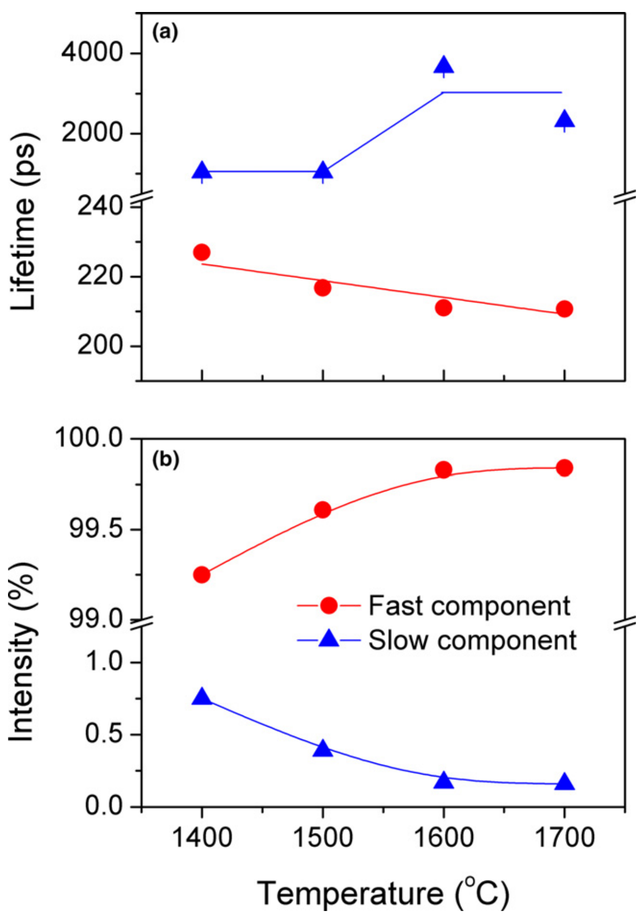

Fig. 2. (a) Lifetimes and (b) relative intensities obtained from PAL measurements of Y_2O_3 pellets sintered at different temperatures. Lines are guides to the eye only.

The radius of the open-volume defects was estimated based on results reported in Ref. [27] and show an increase with sintering temperature, from about 2 to 4 Å, due to the higher mobility of vacancies induced by the higher sintering temperatures. The fast lifetime component is interpreted as being from bulk annihilation with some contribution from grain boundaries and structural disorder in agreement with Ref. [28] where the bulk lifetime of Y_2O_3 was determined to be 200 ps. From Fig. 2(b), it is seen that annihilation is dominated by the fast mechanism, with the relative intensity of the slow mechanism decreasing from ~0.8% to 0.2% for higher temperatures. In summary, PAL results show that the densification of the structure is achieved through the elimination of open-volume defects, as revealed by the decrease in the relative contribution of the slow lifetime and in agreement with density results (Fig. 1), and their progressive agglomeration, as revealed by the increase in the slow lifetime component.

The TL mechanism involves the promotion of electrons to the conduction band (and/or holes to the valence band) followed by their capture by electronic traps close to the edges of the respective band. The traps correspond to the electronic manifestation of defects like vacancies, interstitials, etc. in the form of localized energy levels within the band gap. Thermal energy is used to release charge carriers from the traps, and the recombination of electron and holes at the recombination center may generate TL. Thus, TL measurements are used to gain insight into the presence of electronic traps in yttria. The effects of sintering temperature on the TL of Y_2O_3 were investigated, and Fig. 3 compares typical glow curves from a pellet made of pressed calcined powder and from a pellet of pressed calcined powder that was further sintered at 1400°C. The glow curve from the sintered sample is dominated by a relatively narrow band centered at 100°C, while the glow curve of the calcined sample presents a considerably broader band centered at 140°C with a shoulder at 110°C. The shoulder can possibly correspond to the TL band observed in the case of the sintered sample. It is conceivable that the band shifted to higher temperatures due to the expected lower thermal conductivity of the calcined sample since its density (green density ~50%) is considerably lower than that of the sintered pellet (relative density = 92%). More importantly, in the case of the calcined sample, intense TL emission is observed up to ~250°C that is absent for the sintered sample. These results are in general agreement with TL glow curves of Y_2O_3 commercial powder and nanoparticles reported elsewhere.[29–31] For thermoluminescence to

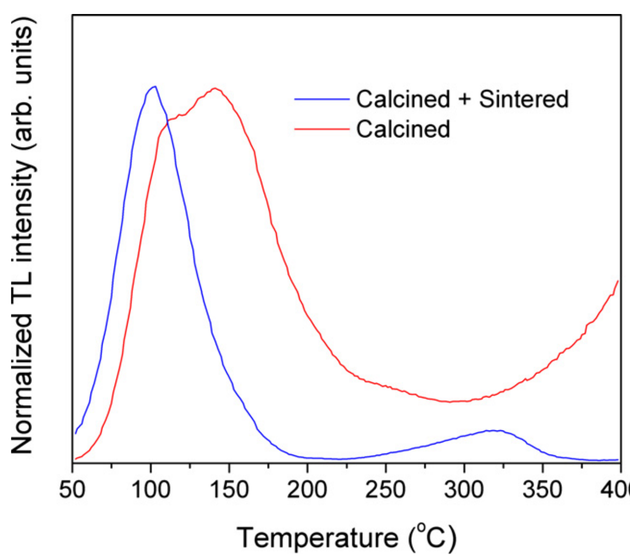

Fig. 3. Normalized TL glow curves of calcined and calcined + sintered pellets.

occur, it is necessary to have at least a trap and a recombination center. While TL results cannot specifically identify the nature of the traps involved, the increase in the peak at 100°C for higher sintering temperatures can be tentatively assigned to the increase in the number of open-volume agglomerates. Further, they suggest that sintering is beneficial in removing traps and/or recombination centers responsible for the emission between about 150°C and 250°C, and for temperatures higher than 350°C. We further investigate how the sintering temperature affects the glow curves. In Fig. 4(a), typical glow curves from pellets sintered at different temperatures are shown together with the average glow curve area value for each temperature [Fig. 4(b)]. While there is no significant change in the shape of the glow curves, the area increases for higher sintering temperatures. These results suggest that higher sintering temperatures do not lead to the creation of new different types of traps and/or recombination centers. However, since for Y_2O_3:Tm transparent ceramics TL signal is inversely related to scintillation output,[17] the higher TL signal caused by higher sintering temperatures is expected to progressive degrade scintillation performance. It is recommended that the lowest sintering temperature that achieves near-full densification should be the best for the fabrication of transparent ceramic scintillators based on Y_2O_3 due to the minimization of TL signal.

(2) Lutetia

The evolution of the density of Lu_2O_3 pellets as a function of the sintering temperature is shown in Fig. 5. A significant increase from 75% to 98% of the reference density (dashed line) can be seen as the temperature increases from 1400°C to 1700°C, in concordance with other reports.[32,33] Analysis of the PAL results revealed the presence of two lifetimes, a fast component in the 204–228 ps range and a slow component within 1269–2174 ps [Fig. 6(a)]. Annihilation is dominated by the fast mechanism whose lifetime decreases from 228 to 204 ps concomitant to an increase in its relative contribution from 99.2% to 99.8% as the sintering temperature increases [Fig. 6(b)]. This lifetime component is ascribed to the bulk contribution, similarly with results of PAL investigation of other sesquioxides, namely Sc_2O_3:Er[16] and Y_2O_3.[28]

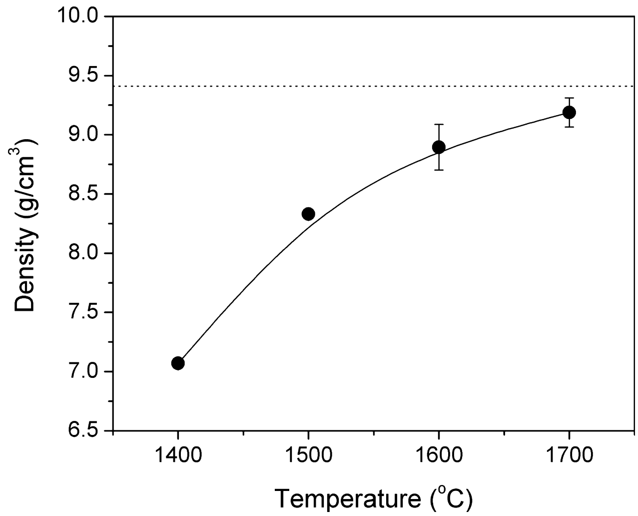

Fig. 5. Density of Lu_2O_3 pellets sintered at different temperatures. Line is a guide to the eye only.

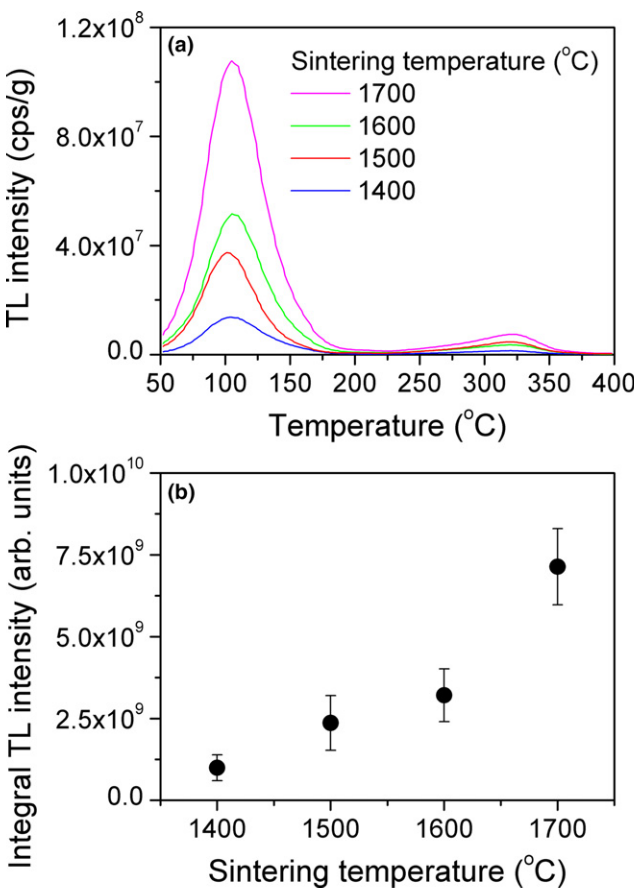

Fig. 4. (a) Representative TL glow curves of Y_2O_3 pellets sintered at different temperatures, and (b) mass-normalized integral TL intensity as a function of sintering temperature.

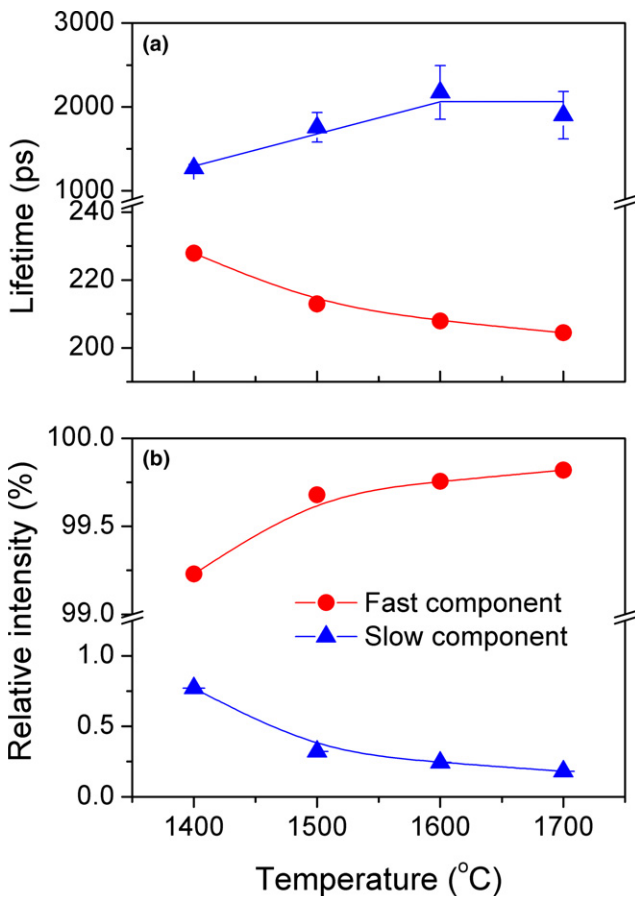

Fig. 6. (a) Lifetimes and (b) relative intensities obtained from PAL measurements of Lu_2O_3 pellets sintered at different temperatures. Lines are guides to the eye only.

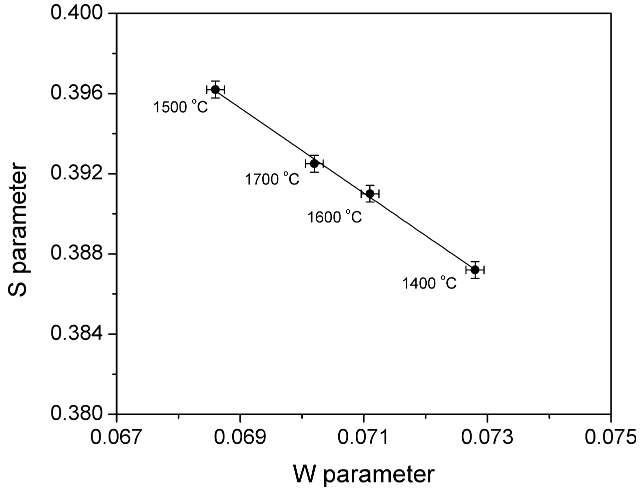

Fig. 7. S × W plot together with linear best fit of the data for Lu_2O_3 samples sintered at different temperatures, as indicated.

However, since full densification of the pellets was not reached even at 1700°C (cf. Fig. 5), neither a clear saturation for the fast component was reached at the highest sintering temperatures [cf. Fig. 6(a)], the lifetime value of 204 ps is interpreted as being from bulk annihilation with some possible contribution from grain boundaries and structural disorder. The slower lifetime is ascribed to positronium annihilation and according to Ref. [27] these results show an increase in the radius of open-volume defects from about 2 to 3 Å for higher sintering temperatures. The near disappearance of the contribution of the slow lifetime component is in agreement with the densification of the pellets as shown by the density measurements (Fig. 5). Like in the case of Y_2O_3, PAL results reveal that densification of the structure (Fig. 5) occurs through the elimination of open-volume defects, as manifested by the decrease in the relative contribution of the slow component that is related to the presence of open-volume defects, as well as the progressive agglomeration of open-volume defects manifested by the increase in the slow lifetime component.

Since no TL signal has been reported for Lu_2O_3,[34] analysis of the broadening of the annihilation photopeak was carried out to gain insight into the nature of the defects present in the lutetia ceramics. Annihilation of positrons occurs mostly after thermalization with the velocity of the electron dominating the relative motion of the electron–positron pair. Consequently, the gamma rays generated in the electron–positron annihilation are Doppler shifted in energy according to the energy of the electron, and the broadening of the annihilation photopeak can be related to the state of the electron. Annihilation with the faster moving core electrons contributes to the wings of the photopeak, while the slower valence electrons contribute to the central region of the photopeak. In this analysis, the photopeak is arbitrarily divided in two regions, wings (W) and central (S), with the relative change in these two areas yielding information about the nature of the open-volume defects. Results of this analysis in the form of the S vs W plot are presented in Fig. 7 for Lu_2O_3 samples sintered at different temperatures together with a linear best fit to the data. Within the error bars, a single straight line is capable of representing all the experimental data showing that the same type of open-volume defect is found in all samples.[23,35,36]

IV. Conclusions

In this work, the effects of different processing steps and processing conditions for the fabrication of Y_2O_3 and Lu_2O_3 ceramics were investigated. It focused on the effects of calcinations, and sintering in the 1400°C–1700°C temperature range on the content of open-volume and electronic defects. Two lifetime components were identified in the PAL analysis. The faster lifetime, 211 ps for Y_2O_3 and 204 ps for Lu_2O_3, was assigned to bulk annihilation with possible contribution of grain boundaries. PAL analysis also showed that densification is achieved through the elimination and agglomeration of open-volume defects. In Y_2O_3, the radius of open-volume defects was estimated to increase from about 2 to 4 Å, while in Lu_2O_3 it increases from about 2 to 3 Å for higher sintering temperatures. Further, in Y_2O_3, it is shown that sintering can be beneficial in decreasing TL signal in the 150°C–250°C region. However, while it is possible to obtain ceramics with relative density of 99% for sintering temperatures ≥1450°C, higher sintering temperatures also lead to higher TL signal. The increase in the TL peak at 100°C for higher sintering temperatures was tentatively assigned to the increase in the number of open-volume agglomerates. It is recommended herein that ceramic scintillators based on Y_2O_3 should be fabricated at the lowest sintering temperature possible to decrease TL signal. In the case of Lu_2O_3, only for the sintering temperature of 1700°C, it was possible to achieve a high relative density of 98% and it was found that the same type of open-volume defect was present regardless the sintering temperature.

Acknowledgments

This material is based upon work supported by the National Science Foundation under Grant No. 1207080. R.C. Walker II acknowledges support from NSF Research Experience for Undergraduates 'Interfaces and Surfaces: Exploring and Experiencing Science' Grant No. 1062873, and J.M. Schmitt acknowledges the Clemson University Calhoun Honors College Experiences in Undergraduate Research, Exploration and Knowledge Advancement (EUREKA!) Program.

References

[1]G. C. Wei, "Transparent Ceramics for Lighting," *J. Eur. Ceram. Soc.*, **29** [2] 237–44 (2009).

[2]P. J. Patel, G. A. Gilde, P. G. Dehmer, and J. W. McCauley, "Transparent Ceramics for Armor and EM Window Applications"; pp. 1–14 in Inorganic Optical Materials II, Proc. SPIE 4102, August 1–3, 2000, San Diego, CA.

[3]V. Lupei, A. Lupei, and A. Ikesue, "Transparent Polycrystalline Ceramic Laser Materials," *Opt. Mater.*, **30** [11] 1781–6 (2008).

[4]J. Li, Y. Pan, Y. Zeng, W. Liu, B. Jiang, and J. Guo, "The History, Development, and Future Prospects for Laser Ceramics: A Review," *Int. J. Refract. Met. Hard Mater.*, **39**, 44–52 (2013).

[5]C. Greskovich C and S. Duclos, "Ceramic Scintillators," *Annu. Rev. Mater. Sci.*, **27**, 69–88 (1997).

[6]D. A. Casano, C. D. Greskovich, and F. A. Dibianca, "Rare-Earth-Doped Yttria-Gadolinia Ceramic Scintillators"; US Patent No. 4,421,671, 1983.

[7]Y. Ito, et al., "Hot Isostatic Pressed Gd_2O_2S-Pr, Ce, F Translucent Scintillator Ceramics for X-ray Computed-Tomography Detectors," *Jpn. J. Appl. Phys.*, Part 2:Lett **27** [8] L1371–3 (1988).

[8]M. Yoshida, et al., "Application of Gd_2O_2S Ceramic Scintillator for X-ray Solid-State Detector in X-ray CT," *Jpn. J. Appl. Phys.* Part 2:Lett **27** [8] L1572–5 (1988).

[9]V. V. Nagarkar, et al., "A New X-Ray Scintillator for Digital Radiography," *IEEE Trans. Nucl. Sci.*, **50** [3] 297–300 (2003).

[10]A. Fukabori, et al., "Optical and Scintillation Characteristics of Y_2O_3 Transparent Ceramic," *J. Appl. Phys.*, **107** [7] 073501 (2010).

[11]A. Fukabori, V. Chani, K. Kamada, F. Moretti, and A. Yoshikawa, "Growth of Tm^{3+}-Doped Y_2O_3, Sc_2O_3, and Lu_2O_3 Crystals by the Micropulling Down Technique and Their Optical and Scintillation Characteristics," *Cryst. Growth Des.*, **11** [6] 2404–11 (2011).

[12]T. Yanagida, et al., "Ultrafast Transparent Ceramic Scintillators Using the Yb^{3+} Charge Transfer Luminescence in RE_2O_3 Host," *Appl. Phys. Exp.*, **4** [12] 126402 (2011).

[13]A. Fukabori, V. Chani, J. Pejchal, K. Kamada, A. Yoshikawa, and T. Ikegami, "Fundamental Optical Constants of Nd-Doped Y_2O_3 Ceramic and Its Scintillation Characteristics," *Opt. Mater.*, **34** [2] 452–6 (2011).

[14]A. Fukabori, et al., "Correlation Between Crystal Grain Sizes of Transparent Ceramics and Scintillation Light Yields," *Ceram. Int.*, **38** [3] 2119–23 (2012).

[15]V. Babin, et al., "Luminescent Properties of RE_2O_3 (RE = Lu, Sc, Y) Single Crystals and Ceramics," *Eur. Phys. J. B*, **86**, 93 (2013).

[16]L. G. Jacobsohn, K. Serivalsatit, C. A. Quarles, and J. Ballato, "Investigation of Er-Doped Sc_2O_3 Transparent Ceramics by Positron Annihilation Spectroscopy," *J. Mater. Sci.*, **50** [8] 3183–8 (2015).

[17]M. G. Chapman, et al., "Luminescence and Scintillation Enhancement of Y_2O_3:Tm Transparent Ceramic Through Post-Fabrication Thermal Processing," *J. Lumin.*, **165**, 56–61 (2015).
[18]L. Wen, X. D. Sun, Q. Lu, G. X. Xu, and X. Z. Hu, "Synthesis of Yttria Nanopowders for Transparent Yttria Ceramics," *Opt. Mater.*, **29** [2–3] 239–45 (2006).
[19]K. Serivalsatit, B. Kokuoz, B. Y. Kokuoz, M. Kennedy, and J. Ballato, "Synthesis, Processing, and Properties of Submicrometer- Grained Highly Transparent Yttria Ceramics," *J. Am. Ceram. Soc.*, **93** [5] 1320–5 (2010).
[20]K. Serivalsatit, T. Wasanapiarnpong, C. J. Kucera, and J. Ballato, "Synthesis of Er-Doped Lu_2O_3 Nanoparticles and Transparent Ceramics," *Opt. Mater.*, **35** [7] 1426–30 (2013).
[21]Joint Committee on Powder Diffraction Standards-International Center for Diffraction Data (JCPDS-ICDD) Card no 41-1105.
[22]International Center for Diffraction Data Powder Diffraction File (ICDD PDF) Card no 01-086-2475.
[23]I. Prochazka, "Positron Annihilation Spectroscopy," *Mater. Struct.*, **8** [2] 55–60 (2001).
[24]J. Kansy, "Microcomputer Program for Analysis of Positron Annihilation Lifetime Spectra," *Nucl. Instrum. Methods Phys. Res., Sect. A*, **374** [2] 235–44 (1996).
[25]M. Urban-Klaehn, R. Spaulding, A. W. Hunt, and E. S. Peterson, "Applicability of the MCNPX Particle Transport Code for Determination of the Source Correction Effect in Positron Lifetime Measurements on Thin Polymer Films," *Phys. Status Solidi C*, **4** [10] 3731–4 (2007).
[26]O. Yeheskel, M. Shokhat, S. Salhov, and O. Tevet, "Effect of Initial Particle and Agglomerate Size on the Elastic Moduli of Porous Yttria (Y_2O_3)," *J. Am. Ceram. Soc.*, **92** [8] 1655–62 (2009).
[27]K. Ito, H. Nakanishi, and Y. Ujihira, "Extension of the Equation for the Annihilation Lifetime of Ortho-Positronium at a Cavity Larger Than 1 nm in Radius," *J. Phys. Chem. B*, **103** [21] 4555–8 (1999).
[28]J. Brown, P. Mascher, and A. H. Kitai, "Positron Lifetime Spectroscopy and Cathodoluminescence of Polycrystalline Terbium-Doped Yttria," *J. Electrochem. Soc.*, **142** [3] 958–60 (1995).
[29]M. S. Jahan, D. W. Cooke, W. L. Hults, J. L. Smith, B. L. Bennett, and M. A. Maez, "Thermally Stimulated Luminescence from Commonly Occurring Impurity Phases in High-Temperature Superconductors," *J. Lumin.*, **47** [3] 85–91 (1990).
[30]R. Hari Krishna, et al., "Auto-Ignition Based Synthesis of Y_2O_3 for Photo- and Thermo-Luminescent Applications," *J. Alloys Compd.*, **585**, 129–37 (2014).
[31]B. N. Lakshminarasappa, N. J. Shivaramu, K. R. Nagabhushana, and F. Singh, "Synthesis Characterization and Luminescence Studies of 100 MeV Si^{8+} ion Irradiated Sol Gel Derived Nanocrystalline Y_2O_3," *Nucl. Instrum. Methods Phys. Res., Sect. A*, **329**, 40–7 (2014).
[32]N. A. Dulina, et al., "Synthesis and Characterization of the Crystalline Powders on the Basis of $Lu_2O_3:Eu^{3+}$ Spherical Submicron-Sized Particles," *J. Eur. Ceram. Soc.*, **30** [7] 1717–24 (2010).
[33]Z. M. Seeley, J. D. Kuntz, N. J. Cherepy, and S. A. Payne, "Transparent Lu_2O_3:Eu Ceramics by Sinter and HIP Optimization," *Opt. Mater.*, **33** [11] 1721–6 (2011).
[34]A. Wiatrowska and E. Zych, "Traps Formation and Characterization in Long-Term Energy Storing Lu_2O_3:Pr,Hf Luminescent Ceramics," *J. Phys. Chem. C*, **117** [22] 11449–58 (2013).
[35]K. Saarinen, P. Hautojarvi, and C. Corbel, "Identification of Defects in Semiconductors"; pp. 209 in *Semiconductors and Semimetals*, Vol. 51A, Edited by M. Stavola. Academic Press, San Diego, 1998.
[36]L. G. Jacobsohn, M. Nastasi, L. L. Daemen, Z. Jenei, and P. Asoka-Kumar, "Positron Annihilation Spectroscopy of Sputtered Boron Carbide Films," *Diamond Relat. Mater.*, **14** [2] 201–5 (2005). □